An Optimized Index Modulation for Filter Bank Multicarrier (FBMC) System

Jian Zhang[1], Minjian Zhao[2], Jie Zhong[3], Pei Xiao[4] and Tianhang Yu[5]

Abstract

Orthogonal frequency division multiplexing with index modulation (OFDM-IM) has attracted considerable interest recently. The technique uses the subcarrier indices as a source of information. In FBMC system, double-dispersive channels lead to inter-carrier interference (ICI) and/or inter-symbol interference (ISI), which are caused by the neighboring symbols in the frequency and/or time domain. When we introduce index modulation to the FBMC system, the interference power will be smaller comparing to that of the conventional FBMC system as some subcarriers carry nothing but zeros. In this paper, the advantages of FBMC with index modulation (FBMC-IM) are investigated by comparing the signal to interference ratio (SIR) with that of the conventional FBMC system. However, the bit error rate (BER) performance is affected since there exists interference in the FBMC-IM system. To improve the BER performance, we propose an optimal combination-selection algorithm and an optimal combination-mapping rule. By abandoning some combinations whose error probability are larger and by mapping the remaining combinations into specified bits, a better BER performance can be achieved compared with that without optimization. The theoretical analysis and simulation results clearly show the FBMC-IM system has a good BER performance under double-dispersive channels.

Index Terms

Index modulation, FBMC, SIR, combination-selection algorithm, combination-mapping rule

I. Introduction

As a promising candidate to realize high data rate transmission in future 5G wireless communication, filter bank multicarrier (FBMC) has recently received significant attention by both academia and industry in the last few years [1], [2]. Different from orthogonal frequency division multiplexing (OFDM), FBMC employs prototype pulses with

J. Zhang, M. Zhao, J. Zhong and T. Yu are with the College of Information Science and Electronic Engineering, Zhejiang University, Hangzhou 310027, China (E-mail: [1] zjfly2008@zju.edu.cn; [2] mjzhao@zju.edu.cn; [3] zhongjie@zju.edu.cn; [5] tianhang0318@zju.edu.cn). P. Xiao is with the Institute for Communications Systems Department of Electronic Engineering, University of Surrey, Guildford, Surrey, GU2 7XH, United Kingdom (E-mail: [4] p.xiao@surrey.ac.uk).

This work is supported by the National Science Foundation of China (NSFC) under Grant 91538103, and the National High Technology Research and Development Program of China (863 Program) under Grant 2014AA01A707.

lower sidelobe and faster spectral decay, which makes FBMC have the advantages of reduced out-of band energy and theoretically higher spectral efficiency [3], [4]. As an another way to improve spectral efficiency, OFDM with index modulation (OFDM-IM) is introduced as a new transmission technique, where the subcarrier indices are bearing information.

Inspired by the concept of spatial modulation in multiple-input multiple-output (MIMO) transmission [5], the authors of [6] proposed OFDM-IM for the first time and laid the foundation for the future series of articles in the filed of OFDM-IM. However, potential bit error propagation became the issue of the OFDM-IM, which could result in significant burst errors. By splitting the subcarriers into some groups, the burst error problem of [6] was solved at the cost of spectral efficiency loss [7] . A low complexity transceiver of OFDM-IM based on maximum likelihood (ML) detection or log-likelihood ratio (LLR) calculation was proposed, which improved the spectral efficiency by selecting more than one active subcarriers [8]. The novel transceiver in [8] lighted the passion of the following researchers. A simple and efficient subcarrier-level interleaving scheme was introduced to improve the BER performance [9]. Then the transceiver in [10] used the concept of splitting orthogonal components of M-ary quadrature amplitude modulation (M-QAM) symbols such that index modulation was applied on the orthogonal components independently, and this resulted in a higher spectral efficiency of OFDM-IM.

Although index modulation is well studied in OFDM, FBMC with index modulation (FBMC-IM) has not been investigated in the literature so far. In this paper, we propose a FBMC-IM model, a combination-selection algorithm and a combination-mapping rule.

We first investigate the advantages of the FBMC-IM system by mathematical analysis of the signal to interference ratio (SIR). In practical scenarios, double-dispersive channels lead to inter-carrier interference (ICI) and/or inter-symbol interference (ISI), which are caused by the neighboring symbols in the frequency and/or time domain [11]. Consequently, the intrinsic orthogonality guaranteed by prototype pulses [12] will be destroyed. As some subcarriers carry nothing but zeros in the proposed FBMC-IM system, the interference power will be smaller comparing to that of the conventional FBMC system and a better SIR will be achieved. The SIR analysis and simulations clearly show that the proposed model has an impressive performance improvement under double-dispersive channels even with channel estimation errors.

However, the interference is not eliminated completely and the remaining interference still affect the performance when we apply index modulation to the FBMC system directly. In order to reduce the remaining interference, we propose an optimal combination-selection algorithm and an optimal combination-mapping rule. By selecting the optimal combinations from all of the combinations, the number of error bits carried by optimal combinations is kept less than that carried by combinations without optimization. After selecting optimal combinations, these

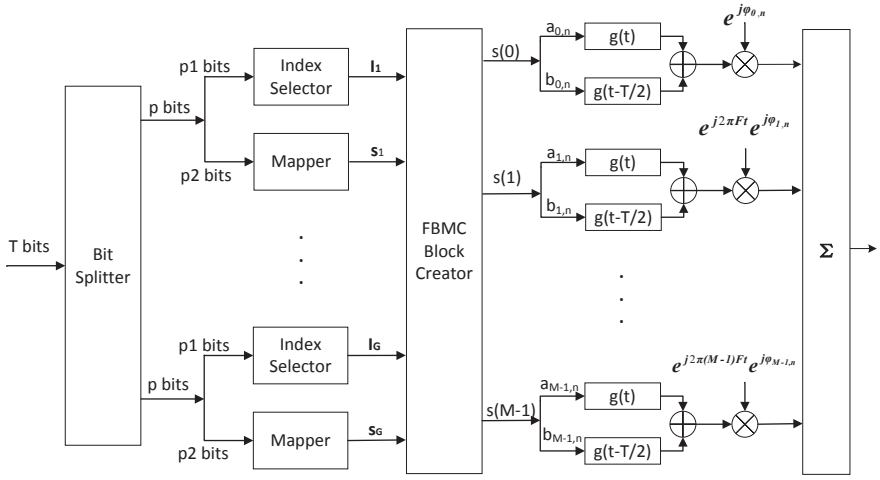

Fig. 1. Block diagram of the FBMC-IM transmitter

combinations are mapped into specified bits by following the optimal combination-mapping rule, and a better performance can be achieved.

The rest of this paper is organized as follows. Section II gives a mathematical description of the proposed FBMC-IM model. In Section III, we give the advantages of the FBMC-IM system in terms of SIR. Then the BER performance improvement of the FBMC-IM system by applying the optimal combination-selection algorithm and optimal combination-mapping rule is presented in section IV and section V. Simulation results of the FBMC-IM system are presented in Section VI. Finally, Section VII concludes the paper.

II. SYSTEM MODEL OF FBMC-IM

In FBMC-IM system, we define the subcarriers bearing constellation symbols as active ones, and the subcarriers left blank as inactive ones, correspondingly. The modulating model of FBMC-IM system is illustrated in Fig.1.

In this model, the transmitted information of each block are T bits. The M subcarriers are divided into G groups, with Q subcarriers for each group, i.e., $M = QG$. Let us assume that each group contains p bits, which can be split into two parts. The first p_1 bits are fed to the index selector and k out of Q subcarriers are activated according a look-up table [8] while the remaining p_2 bits are mapped to the activated k constellation symbols. Therefore, the number of bits carried by the indices of subcarriers is given by

$$p_1 = \lfloor \log_2 C_Q^k \rfloor, \tag{1}$$

where $\lfloor x \rfloor$ is the greatest integer smaller than x and C_Q^k denotes the binomial coefficient. The number of bits carried by the constellation symbols is given by

$$p_2 = k(\log_2 N), \tag{2}$$

where N stands for a N-ary signal constellation. In general, the transmitted bits in each group are $p_1 + p_2$, and the total number of bits that can be transmitted by one FBMC block is

$$T = (p_1 + p_2)G. \tag{3}$$

After modulation, the subblock can be written as

$$\mathbf{S}_g = [0, ..., S_{g,0}, 0, ..., 0, S_{g,1}, 0, ..., 0, ...S_{g,k-1}, ..., 0]^T_{Q\times 1} \tag{4}$$

where $S_{g,i}(i = 0, 1, ..., k-1)$ denotes the N-ary constellation symbol, and $\mathbf{S}_g \in \Lambda$, where Λ is the set of all possible signal vectors. After that, the subblock symbols are sent to the FBMC block creator, which can be implemented either by a consecutive way [8] or by an interleaved way [9]. The symbol after FBMC block creator is described as

$$\mathbf{S}_M = [s_M(0), s_M(1), ..., s_M(M-1)]^T_{M\times 1} \tag{5}$$

where $s_M(m) = a_m + jb_m(m = 0, 1, 2, ..., M-1)$. a_m and b_m are the real and imaginary part of $s_M(m)$.

After FBMC modulation, the FBMC-IM signal can be written as follows:

$$s(t) = \sum_{m=0}^{M-1}\sum_{n=0}^{+\infty} e^{j2\pi mFt} e^{j\phi_{m,n}} \{a_{m,n} g(t - nT) + jb_{m,n} g(t - \frac{T}{2} - nT)\}, \tag{6}$$

where n, m and M are the time index for the input FBMC-IM symbol, the index of subcarrier and the total number of subcarriers respectively. $F = 1/T$ is the subcarrier spacing and $g(t)$ is the symmetric prototype filter. $a_{m,n}$ and $b_{m,n}$ are the real and imaginary part of $s(m)$ when time index is n. We assume that $a_{m,n}$ and $b_{m,n}$ are independent and identically distributed with $E\{a_{m,n}\} = E\{b_{m,n}\} = 0$ and $E\{|a_{m,n}|^2\} = E\{|b_{m,n}|^2\} = \sigma_s^2/2$ for all the value of m and n. $\phi_{m,n}$ is an additional phase term which can be expressed as $\frac{\pi}{2}m$ [1]. In (6), the real part $a_{m,n}$ and imaginary part $b_{m,n}$ are always non-zero when the active subcarrier number k is equal to Q in each subblock, which also corresponds to the conventional FBMC system. As a result, the conventional FBMC system can be viewed as a special case of the FBMC-IM system.

The transmit signals $s(t)$ will pass through a multi-path fading channels with a carrier frequency offset f_d. A general channel model can be expressed in continuous-time as

$$h(t, \tau) = \sum_{i=0}^{L-1} c_i e^{j2\pi f_d t} \delta(\tau - \tau_i), \tag{7}$$

where L is the number of path and c_i is the time-varying channel gain to the i-th path. τ_i denotes the time delay of the i-th path and δ represents the Dirac delta function.

Combining (6) and (7), the received FBMC-IM signal with AWGN noise and channel fading can be given by,

$$\begin{aligned} y(t) &= \sum_{i=0}^{L-1} h(t,\tau_i)s(t-\tau_i) + n(t) \\ &= \sum_{i=0}^{L-1} c_i e^{j2\pi f_d t} \sum_{m=0}^{M-1}\sum_{n=0}^{+\infty} e^{j2\pi mF(t-\tau_i)} e^{j\phi_{m,n}} \{a_{m,n}g(t-nT-\tau_i) + jb_{m,n}g(t-\frac{T}{2}-nT-\tau_i)\} + n(t). \end{aligned} \tag{8}$$

Note that the intrinsic interference to neighborhoods caused by the channel delay τ_i and carrier frequency offset f_d will not exist when $a_{m,n}$ and $b_{m,n}$ are zero in the proposed FBMC-IM system. As a result, the performance will be obviously improved in the FBMC-IM system. In the next section, the detailed analysis will be presented.

III. FBMC-IM PERFORMANCE ANALYSIS ON SIR

In this section, the advantages of the FBMC-IM system are analyzed in detail. We first separate the demodulated symbol into the useful signal part and the interference part. Then some approximations are taken to make it possible to calculate the power of the signal and the interference. And the performance of the FBMC-IM system will be analyzed in terms of SIR finally.

A. The derivation of the demodulated symbol

At the receiver, the received signal passes through the filters. Assume the one-tap equalizer coefficients as ω_{m_0,n_0} at the (m_0, n_0) position, then the real and imaginary part of demodulated signal at the (m_0, n_0) position are given by

$$\begin{aligned} \hat{a}_{m_0,n_0} &= \Re\{\omega_{m_0,n_0} \underbrace{\int_{-\infty}^{+\infty} y(t)g^*(t-n_0T)e^{-j(2\pi m_0 Ft+\phi_{m_0,n_0})}dt}_{A_{m_0,n_0}}\}, \\ \hat{b}_{m_0,n_0} &= \Im\{\omega_{m_0,n_0} \underbrace{\int_{-\infty}^{+\infty} y(t)g^*(t-\frac{T}{2}-n_0T)e^{-j(2\pi m_0 Ft+\phi_{m_0,n_0})}dt}_{B_{m_0,n_0}}\}. \end{aligned} \tag{9}$$

Then the estimated symbol can be expressed as $\hat{s}_{m_0,n_0} = \hat{a}_{m_0,n_0} + j\hat{b}_{m_0,n_0}$. Substituting (8) into (9), and omitting the noise term, the A_{m_0,n_0} part of the demodulated signal $\hat{a}_{m_0,n_0}$ can be obtained as

$$\begin{aligned} A_{m_0,n_0} = \int_{-\infty}^{+\infty} &\sum_{i=0}^{L-1} c_i e^{j2\pi f_d t} \sum_{m=0}^{M-1}\sum_{n=0}^{+\infty} e^{\phi_{m,n}-\phi_{m_0,n_0}} \\ &\times (a_{m,n}g(t-nT-\tau_i) + jb_{m,n}g(t-\frac{T}{2}-nT-\tau_i))g^*(t-n_0T)e^{j2\pi mF(t-\tau_i)}e^{-j2\pi m_0 Ft}dt. \end{aligned} \tag{10}$$

In FBMC system, we define the ambiguity function as

$$A_g(\tau,\upsilon) = \int_{-\infty}^{+\infty} g(t+\frac{\tau}{2})g^*(t-\frac{\tau}{2})e^{j2\pi\upsilon t}dt. \tag{11}$$

Then (10) can be simplified as

$$\begin{aligned} A_{m_0,n_0} = &\sum_{m=0}^{M-1}\sum_{n=0}^{+\infty} a_{m,n}e^{j\phi_1}\sum_{i=0}^{L-1} c_i e^{j\phi_2} A_g[(n_0-n)T-\tau_i,(m_0-m)F-f_d] \\ &+\sum_{m=0}^{M-1}\sum_{n=0}^{+\infty} jb_{m,n}e^{j\phi_1}\sum_{i=0}^{L-1} c_i e^{j\phi_3} A_g[(n_0-n)T-\frac{T}{2}-\tau_i,(m_0-m)F-f_d], \end{aligned} \tag{12}$$

where $\phi_1 = \phi_{m,n} - \phi_{m_0,n_0}$, ϕ_2 can be expressed as

$$\phi_2 = \pi[(m-m_0)F_0 + f_d][(n+n_0)T+\tau_i] - 2\pi m F_0 \tau_i \tag{13}$$

and ϕ_3 can be expressed as

$$\phi_3 = \pi[(m-m_0)F_0 + f_d][(n+n_0)T+\frac{T}{2}+\tau_i] - 2\pi m F_0 \tau_i. \tag{14}$$

It is assumed that $m = m_0 + p, n = n_0 + q, T = MT_s$ and $A_g[q,p] = A_g[qT_s, pF]$. r indicates the normalized doppler shift which denotes $r = f_d T$ and l means the l-th path of the fading channel. With a digitization step, we can obtain the demodulated symbol A_{m_0,n_0} which can be expressed as

$$A_{m_0,n_0} = \sum_{(p,q)} (a_{m_0+p,n_0+q}E_{m_0,n_0} + jb_{m_0+p,n_0+q}F_{m_0,n_0}) \tag{15}$$

with

$$E_{m_0,n_0} = \sum_{l=0}^{L-1} c_l e^{j\pi(2n_0p+pq-\frac{p}{2})} e^{j\pi(2n_0+q+\frac{l}{M})r} A_g[-qM-l,-p-r] e^{-j\pi(2m_0+p)\frac{l}{M}} \tag{16}$$

$$F_{m_0,n_0} = \sum_{l=0}^{L-1} c_l e^{j\pi(2n_0p+pq)} e^{j\pi(2n_0+q+\frac{l}{2}+\frac{l}{M})r} A_g[-qM-\frac{M}{2}-l,-p-r] e^{-j\pi(2m_0+p)\frac{l}{M}}. \tag{17}$$

Similarly, the demodulated symbol B_{m_0,n_0} can be expressed as

$$B_{m_0,n_0} = \sum_{(p,q)} (jb_{m_0+p,n_0+q}E_{m_0,n_0} + a_{m_0+p,n_0+q}F_{m_0,n_0}). \tag{18}$$

$\Omega_{m,n}$ is defined as the neighborhoods of (m_0,n_0) and $\Omega^*_{m,n} = \Omega_{m,n} - \{(0,0)\}$, which means the neighborhood of (m_0,n_0) except the central position. Therefore, the demodulated data symbol at the (m_0,n_0) position can be written as

$$\hat{s}_{m_0,n_0} = \Re\{\omega_{m_0,n_0} \underbrace{\sum_{l=0}^{L-1} c_l e^{-j2\pi m_0\frac{l}{M}} e^{j\pi(2n_0+\frac{l}{M})r} A_g[-l,-r]}_{\alpha_{m_0,n_0}}\}(a_{m_0,n_0}+jb_{m_0,n_0}) + I_{m_0,n_0}, \tag{19}$$

where

$$\begin{aligned} I_{m_0,n_0} = &\Re\{\sum_{\Omega^*_{m,n}} \omega_{m_0,n_0} a_{m_0+p,n_0+q} E_{m_0,n_0}\} + \Re\{\sum_{\Omega_{m,n}} \omega_{m_0,n_0} j b_{m_0+p,n_0+q} F_{m_0,n_0}\} \\ &+ j\Im\{\sum_{\Omega_{m,n}} \omega_{m_0,n_0} a_{m_0+p,n_0+q} F_{m_0,n_0}\} + j\Im\{\sum_{\Omega^*_{m,n}} \omega_{m_0,n_0} j b_{m_0+p,n_0+q} E_{m_0,n_0}\} \end{aligned} \tag{20}$$

B. The analysis of SIR in the FBMC-IM system

As a measure of the performance analysis, we define the SIR as

$$SIR = \frac{P_s}{P_I}, \tag{21}$$

where P_s and P_I are the desired symbol power and the interference power.

We assume that the estimation of the channel is not accurate. The remaining doppler frequency f_d can be viewed as channel estimation error but the value of f_d is small compared with F, which means $r \ll 1$. Besides, it is assumed that the number of subcarriers M is very large compared with the maximum delay of the channel, which means that $L \ll M$. Based on these assumption, we can simplify the estimated data symbol by making the following observations:

- Due to the fact that $r \ll 1$ and $L \ll M$, $\frac{l}{M} r$ is small enough to guarantee that the approximation $e^{j\frac{l}{M}r} \approx 1$ holds.
- Since the maximum delay of the channel satisfies $L \ll M$ and $A_g[0,0] \approx A_g[L,0]$ according to the property of the ambiguity function [13], we can replace $A_g[l,0]$ as $A_g[L/2,0]$.
- The channel frequency response without doppler frequency at the (m_0, n_0) position can be defined as $H_{m_0,n_0} = \sum_{l=0}^{L-1} c_l e^{-j2\pi m_0 \frac{l}{M}}$, which can also be regarded as the estimated channel response.
- With $n_0 \in \mathbf{N}$ and $p \in \mathbf{N}$, we obtain $e^{j2\pi n_0 p} = 1$.
- The prototype pulse is well localized in time and frequency, which contributes to the interference mainly coming from the small size neighborhood around. We only consider the first-order neighborhood and second-order neighborhood to compute the interference term.
- Since the channel is slow-fading, we can conclude that $H_{m_0,n_0} \approx H_{m_0+\frac{p}{2},n_0}$.

With the help of the above observations, α_{m_0,n_0}, M and N can be simplified as

$$\alpha_{m_0,n_0} = H_{m_0,n_0} e^{j2\pi n_0 r} A_g[-L/2, -r], \tag{22}$$

$$E_{m_0,n_0} \approx H_{m_0,n_0} e^{j\pi(pq-\frac{p}{2})} e^{j\pi(2n_0+q)r} A_g[-qM - \frac{L}{2}, -p-r] \tag{23}$$

and

$$F_{m_0,n_0} \approx H_{m_0,n_0} e^{j\pi pq} e^{j\pi(2n_0+q+\frac{1}{2})r} A_g[-qM - \frac{M}{2} - \frac{L}{2}, -p-r]. \tag{24}$$

Before taking the real part (or imaginary part) of the demodulated symbol, a simple one-tap zero-forcing (ZF) equalizer should be employed to compensate the effect of the channel, which means $\omega_{m_0,n_0} = H_{m_0,n_0}$. The estimated data symbol after equalizer can be expressed as

$$\begin{aligned}\hat{s}_{m_0,n_0} = &\Re\{\frac{\alpha_{m_0,n_0}}{H_{m_0,n_0}}\}(a_{m_0,n_0} + jb_{m_0,n_0}) + \Re\{\sum_{\Omega^*_{2,2}} a_{m_0+p,n_0+q}\frac{E_{m_0,n_0}}{H_{m_0,n_0}}\} \\ &+ \Re\{\sum_{\Omega_{2,2}} jb_{m_0+p,n_0+q}\frac{F_{m_0,n_0}}{H_{m_0,n_0}}\} + j\Im\{\sum_{\Omega_{2,2}} a_{m_0+p,n_0+q}\frac{F_{m_0,n_0}}{H_{m_0,n_0}}\} + j\Im\{\sum_{\Omega^*_{2,2}} jb_{m_0+p,n_0+q}\frac{E_{m_0,n_0}}{H_{m_0,n_0}}\}.\end{aligned} \tag{25}$$

Then the desired signal power can be written as

$$P_s = \sigma_s^2 A_g^2[-L/2, -r]\cos^2(2n_0 r\pi). \tag{26}$$

From (26), we could find that the degradation comes from the doppler frequency and channel delay. The interference power can be calculated as

$$\begin{aligned}P_I = &\frac{\sigma_s^2}{2}\sum_{\Omega^*_{2,2}}\cos^2(\phi_4)A_g^2[-qM - \frac{L}{2}, -p-r] + \frac{\sigma_s^2}{2}\sum_{\Omega_{2,2}}\cos^2(\phi_5+\frac{\pi}{2})A_g^2[-qM - \frac{M}{2} - \frac{L}{2}, -p-r] \\ &+ \frac{\sigma_s^2}{2}\sum_{\Omega_{2,2}}\sin^2(\phi_5)A_g^2[-qM - \frac{M}{2} - \frac{L}{2}, -p-r] + \frac{\sigma_s^2}{2}\sum_{\Omega^*_{2,2}}\sin^2(\phi_4+\frac{\pi}{2})A_g^2[-qM - \frac{L}{2}, -p-r],\end{aligned} \tag{27}$$

where

$$\phi_4 = (pq - p/2 + 2n_0 r + qr)\pi, \tag{28}$$

$$\phi_5 = (pq + r/2 + 2n_0 r + qr)\pi. \tag{29}$$

Each of the interference power item is a positive summation of the small size neighborhoods around the central. Different from the conventional FBMC system, not all of the subcarriers are active in our FBMC-IM system and the inactive subcarriers carry nothing. In other words, only the active subcarriers make contribution to the interference power, which results in lower interference power and higher SIR in FBMC-IM system. With higher SIR in the proposed FBMC-IM system, it has a better performance when using the ML detector to optimally detect the transmit signal compared with that of the conventional FBMC system.

IV. THE OPTIMAL COMBINATION-SELECTION ALGORITHM

For the FBMC-IM system, not all of the combinations are used to carry bits by the indices of subcarriers when $\log_2 C_Q^k > \lfloor \log_2 C_Q^k \rfloor$, which leads us to select the optimal combinations to achieve a better performance. In this section, the optimal selection algorithm is presented.

A. Motivation

For the active subcarrier decoding error, we take $(Q, k) = (6, 3)$ for example to expound the two error types. A combination is chosen randomly which is shown in Fig.2.A. In this figure, $\times$ stands for the active part and $\diamond$ represents the inactive one. a is the in-phase component and b means the quadrature component. The number on the right side of the subcarrier is the subcarrier index of this group.

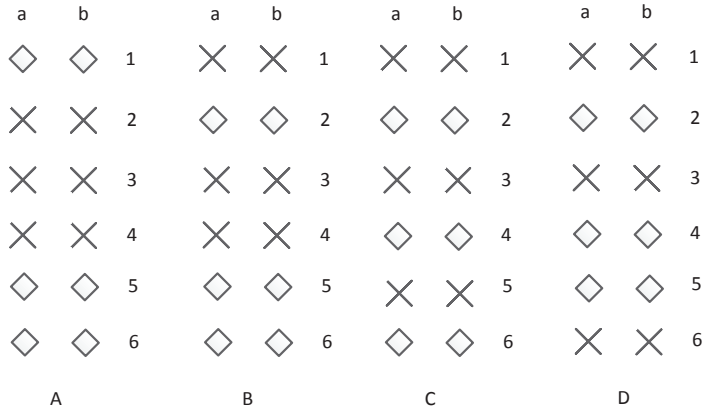

Fig. 2. Four kinds of combinations when $(Q, k) = (6, 3)$

The first error type is expressed that the active subcarriers are decoded wrong while the indices of the active and inactive subcarriers are decoded right. This means that the bits carried in subcarrier 2,3 and 4 are decoded wrong because of the noise and the interference from other subcarriers. This error type can't be avoided.

The second error type is expressed that the indices of the active and inactive subcarriers are decoded wrong. The active subcarrier 3 may be decoded into an inactive one and the inactive subcarrier 1 may be decoded into an active one. This can be regarded as the inactive subcarrier 1 and the active subcarrier 3 are in a reverse order. When the constellation symbols are decoded, it is decoded in an order of 124 instead of 234 because of the wrong decoded index. In this case, the number of error symbols is at least 2. The relationship between the wrong decoding index and the number of error symbols is shown in table I, where only one active subcarrier and one inactive subcarrier are in a reserve order. From this table, we can see that the error symbol number is the maximum when all of the active subcarrier indices are out of order compared with the original active subcarrier indices. This is the case that we should avoid.

TABLE I
THE RELATIONSHIP BETWEEN THE WRONG DECODING INDEX AND THE ERROR BITS NUMBER IN FIG.2.A

original active subcarrier index	reserve order	wrong decoding index	error symbol number
234	$2 \leftrightarrow 1$	134	1
234	$2 \leftrightarrow 5$	345	3
234	$2 \leftrightarrow 6$	346	3
234	$3 \leftrightarrow 1$	124	2
234	$3 \leftrightarrow 5$	245	2
234	$3 \leftrightarrow 6$	246	2
234	$4 \leftrightarrow 1$	123	3
234	$4 \leftrightarrow 5$	235	1
234	$4 \leftrightarrow 6$	236	1

B. The optimal combination-selection algorithm

To compare the error probability with each other, we choose four kinds of combinations illustrated in Fig.2. We only consider the case that one active subcarrier and one inactive subcarrier are in a reserve order. For combination A, all of the active subcarrier indices are out of order and this error probability is $3/9$ (the total number of the wrong decoding indices is 9) when the reserve order are $2 \leftrightarrow 5$,$2 \leftrightarrow 6$ and $4 \leftrightarrow 1$. For combination B, this error probability is $2/9$ by the same analysis when the reserve order are $1 \leftrightarrow 5$ and $1 \leftrightarrow 6$. This error probability of combination C is $1/9$ when the reserve order is $1 \leftrightarrow 6$. And this error probability of combination D is 0.

From the analysis of the probability of the wrong decoding index, we can draw the following conclusion: when only one active subcarrier and one inactive subcarrier are in a reserve order, it might make all of the active subcarrier indices out of order. This error probability is proportional to the number of the inactive subcarriers which are outside of the first active subcarrier and the last active subcarrier. This conclusion is illustrated in table II.

TABLE II
THE RELATIONSHIP BETWEEN THE PROBABILITY AND THE NUMBER OF ELIGIBLE INACTIVE SUBCARRIERS

combination index	the number of eligible inactive subcarriers	the error probability
A	3	$3/9$
B	2	$2/9$
C	1	$1/9$
D	0	0

It is very important for us to abandon the combination that has a larger error probability when only one active subcarrier and one inactive subcarrier are in a reserve order. According to the above conclusion, the combination-selection algorithm can be depicted in the follows:

- When the number of the redundant combinations($\log_2 C_Q^k - \lfloor \log_2 C_Q^k \rfloor$) is equal to the number of the combinations whose error probability (making all of the active subcarrier index out of order) are the largest, then we abandon the combinations whose error probability are the largest. For example, when $(Q, k) = (6, 3)$,

the number of the redundant combinations is 4, and the number of the combinations whose error probability are the largest is also 4. Then we abandon these 4 combinations and the remaining 16 combinations are just enough to carry 4 bits information.

- When the number of the redundant combinations is more than the number of the combinations whose error probability are the largest, the difference should be filled up with the combinations whose error probability are the second largest. For example, When $(Q, k) = (8, 4)$, there exist $C_8^4 = 70$ combinations and only 64 combinations are used to carry 6 bits information. However, only 5 combinations have the largest error probability. We should pick out and abandon another one combination whose error probability are the second largest.
- When the number of the redundant combinations is less than the number of the combinations whose error probability are the largest, we only abandon the required number of combinations from the largest error probability combinations. The selecting rule will be described in section V. For example, On the case of $(Q, k) = (4, 2)$, there are 3 combinations whose error probability are the largest. However, the remaining 3 combinations are insufficient to carry 2 bits information. In this case, we only abandon 2 combinations to transfer 2 bits information with the remaining 4 combinations.

C. BER improvement

Assume that only one active subcarrier and one inactive subcarrier are in a reserve order, the mathematical expectation for the number of error symbols in each combination can be expressed as

$$E(Error\_N) = \sum_{i=1}^{N_e} ik_iP / \sum_{i=1}^{N_e} k_i \tag{30}$$

where P is the probability of one active subcarrier and one inactive subcarrier being in a reserve order, N_e is the maximum error symbol number. $k_i (i = 1, 2, \ldots, N_{e1})$ is the number of i active subcarriers being reverse order. And $Pk_i / \sum_{i=1}^{N_{e1}} k_i$ can be regarded as the probability of i active subcarriers being reverse order.

For each combination when Q and k are selected, the total number of item N_e is the same, the result of $\sum_{i=1}^{N_e} k_i$ is the same, and the probability P is the same. From the optimal selection algorithm depicted in section IV-B, the abandoned combinations have the largest error probability, which means that the number k_{N_e} of the abandoned combinations is larger than that of the remaining combinations. And the summation $\sum_{i=1}^{N_{e1-1}} k_i$ of the abandoned combinations are less than that of the remaining combinations. As N_e is the maximum error symbol number, then the abandoned combinations have a larger mathematical expectation compared with that of the remaining combinations according to (30). When only one active subcarrier and one inactive subcarrier are in a reserve order, a better BER performance can be achieved by abandoning the combinations whose have the largest mathematical

expectation for error symbol number.

The above description only considers the case that one active subcarrier and one inactive subcarrier are in a reserve order. This can be called case A. And there exists the case that more than one active subcarriers and more than one inactive subcarriers are in reserve orders. This can be called case B. The case B can be regarded as an extension of the case A. However, the number of error bits caused by the case B is not the summation of the error bits caused by case A occurs respectively. Actually, the number of error bits caused by case B is less than the summation of the error bits caused by case A occurs respectively. As a result, case A is the key point which affects the BER performance. So we only considers the case that one active subcarrier and one inactive subcarrier are in a reserve order. And the optimal combination selection algorithm show its superiority when case A occurs.

Take $(Q, k) = (6, 3)$ for example. We can calculate the mathematical expectation of each combination in Fig.2 as follows,

$$\begin{aligned} E_A(Error\_N1) &= 1/9 \times \{3 \times 1 + 3 \times 2 + 3 \times 3\} = 18/9, \\ E_B(Error\_N1) &= 1/9 \times \{4 \times 1 + 3 \times 2 + 2 \times 3\} = 16/9, \\ E_C(Error\_N1) &= 1/9 \times \{5 \times 1 + 3 \times 2 + 1 \times 3\} = 14/9, \\ E_D(Error\_N1) &= 1/9 \times \{6 \times 1 + 3 \times 2\} = 12/9. \end{aligned} \tag{31}$$

Obviously, the abandoned combination A has the largest mathematical expectation for the number of error symbols.

V. THE OPTIMAL COMBINATION-MAPPING RULE

After selecting the optimal combinations, the next step is mapping the combinations into bits according to a look-up table. However, the mapping is not performed randomly. The BER performance can be improved if the mapping follows a rule. In this section, the optimal combination-mapping rule is presented.

A. Motivation

Similar to the optimal combination-selection algorithm, we take $(Q, k) = (4, 2)$ for example and choose three combinations randomly which is shown in Fig.3 to demonstrate how to map the combinations. If we encode the symbol in these combinations with the rule that the active subcarrier is encoded to 1 and the inactive subcarrier is encoded to 0, then these three combinations can be encoded as $[0101]$, $[1001]$ and $[1010]$. The number of bits carried by the indices of subcarrier is 2. Each combination in Fig.3 can be mapped into 00, 01, 10 or 11. In this section, we only consider the bits carried by the indices of subcarrier.

If the first combination is mapped into 00 and the second one is mapped into 11, the number of error bits carried by the indices of subcarrier is 2 when the first combination is wrongly decoded into the second one. Similarly, if

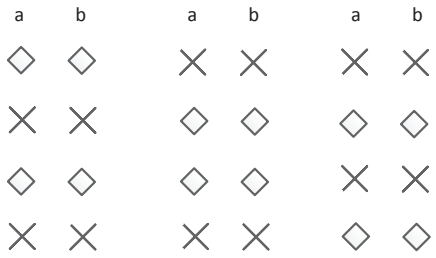

Fig. 3. Three kinds of combinations when $(Q, k) = (4, 2)$

the first combination is mapped into 00 and the last one is mapped into 11, the number of error bits is 2 when the same error happens. However, it is more difficult for the first combination being wrongly decoded into the last one than the first combination being wrongly decoded into the second one, because the Hamming distance between the first combination and the second one is 2 while the Hamming distance between the first combination and the last one is 4. Then we can map the first combination into 00, the second combination into 10 and the last one into 11, respectively. When one active subcarrier and one inactive subcarrier are in a reserve order, only 1 bit information is decoded wrong. The case that 2 bits information are decoded wrong happens when all of the active subcarriers and inactive subcarriers are in reserve orders.

B. The optimal combination-mapping rule

The above analysis indicates that we can achieve a better BER performance by mapping the combinations into specified bits. And the mapping rule can be described that the larger the Hamming distance between the original combinations is, the larger the Hamming distance between the mapping corresponding bits is. The Gray code constellation is used to map the combinations to specified bits. The mapping rule is illustrated in the follows by going on taking $(Q, k) = (4, 2)$ for example.

Step1: List the 16-QAM Gray code constellation which is illustrated in Fig.4.a.

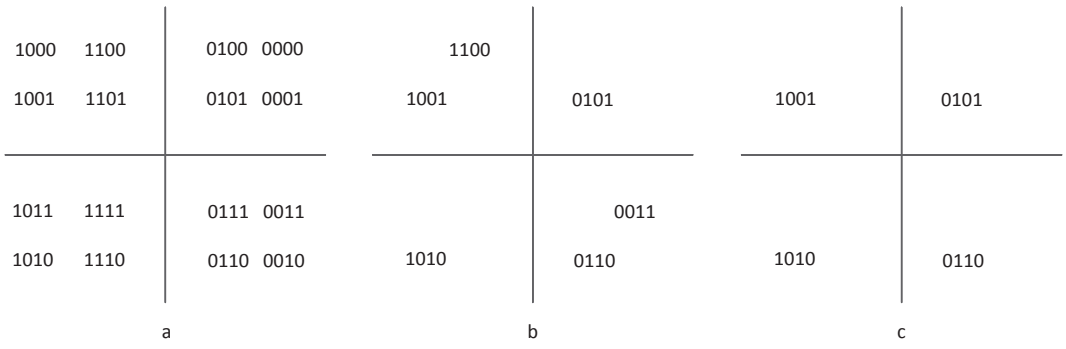

Fig. 4. The procedure of the Gray code constellation optimization

Step2: According to the rule that the active subcarrier is encoded to 1 and the inactive subcarrier is encoded to 0, each combination contains two 1s and two 0s when $(Q, k) = (4, 2)$. So we remove the constellation points whose

signal contents are not two 1s and two 0s. The Gray code constellation after removing is shown in Fig.4.b. The remaining six constellation points are corresponding with the six combinations.

Step3: Combined with the combination-selection algorithm in section IV, we abandon the redundant combinations. In this example, we should abandon 2 combinations although the number of the largest error probability combinations is 3. Following the maximize the Hamming distance of all of the remaining combinations, we abandon the combination $[1100]$ in the second quadrant and the combination $[0011]$ in the fourth quadrant. The Gray code constellation after abandoning the combinations is shown in Fig.4.c.

Step4: Map the 4 optimized combinations into 2 bits Gray code. The mapping process is shown in Fig.5.

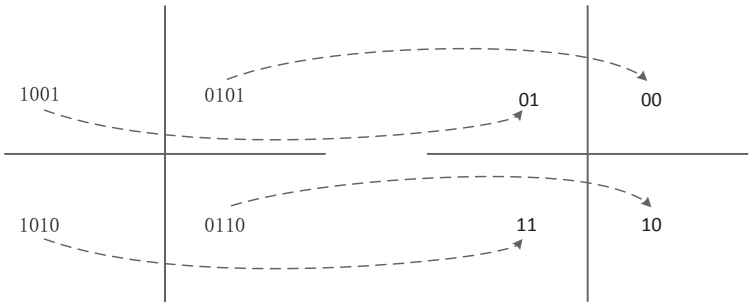

Fig. 5. The mapping process

In general, the process of the optimal combination-mapping rule is shown as follows:

Step1: List the 2^Q-QAM Gray code constellation.

Step2: Remain the constellation points which meet the conditions that the number of one is k and the number of zero is $Q-k$. Remove the other constellation points.

Step3: Abandon the required number of combinations from the largest error probability combinations by following both the optimal combination-selection algorithm in section IV and the rule that maximize the Hamming distance of the remaining combinations.

Step4: Map the remaining combinations into corresponding p_1 bits Gray code.

C. BER improvement

With Gray code bit mapping, the BER performance is independent of the transmitted combinations. Hence, without loss of generality, we will select one combination in the first quadrant which is mapped into 0 as the transmitted combination.

Assume that the probability of active subcarrier being wrongly decoded into inactive one or the inactive subcarrier being wrongly decoded into active one in each combinations is $P(0 < P < 1)$. Then the probability of the

transmitted combination being incorrectly decoded is expressed as

$$P_s = \sum_{i=1}^{N_c} A_i, \tag{32}$$

where $N_c = 2^{p_1} - 1$ represents that the number of the combinations minus one. $A_i = P^{\alpha}$, with α being the Hamming distance between the transmitted combination and the other combinations. Then we have the following expression for average BER

$$P_b = \frac{1}{p_1} \sum_{i=1}^{N_c} W_i A_i, \tag{33}$$

where W_i is the Hamming distance between the bits mapped by the transmitted combination and the bits mapped by the other combinations.

When Q and k are selected, the summation item $\frac{1}{p_1} \sum_{i=1}^{N_c} W_i$ for different mapping rule is the same. From the optimal combination-mapping rule depicted in section V-B, the larger the Hamming distance between the original combinations denotes a larger α, and the larger the Hamming distance between the mapping corresponding bits represents a larger W_i. That is to say, when α is large, the item W_i in the front of P^{α} by following the optimal mapping rule is larger than that by mapping randomly. As the summation item $\frac{1}{p_1} \sum_{i=1}^{N_c} W_i$ is a constant, when α is small, the item W_i in the front of P^{α} by following the optimal mapping rule is smaller than that by mapping randomly. For the reason of $0 < P < 1$, then the P_b by following the optimal mapping rule is smaller than that by mapping randomly. And for a smaller P, the superiority of the optimal mapping rule is more obvious.

Take $(Q, k) = (4, 2)$ as an example. The average BER by following the optimal mapping rule is

$$P_{b\_op} = \frac{1}{2}(2P^2 + 2P^4). \tag{34}$$

While BER by the mapping randomly is

$$P_{b\_wp} = \frac{1}{2}(3P^2 + P^4). \tag{35}$$

Then we can calculate the difference

$$P_{b\_op} - P_{b\_wp} = \frac{1}{2}P^2(P^2 - 1) < 0. \tag{36}$$

VI. SIMULATION RESULTS

In this section, simulations are carried out to validate the performance of the proposed FBMC-IM system and the optimization algorithm. The main parameters of the system used are listed below:

- Sample rate: $F_s = 15.36Msps$

TABLE III
SIR IMPROVEMENT OF THE FBMC-IM SYSTEM

$Mode$	QPSK				8PSK				
(Q,k)	$(4,1)$	$(4,2)$	$(4,3)$	$(4,4)$/FBMC	$(4,1)$	$(4,2)$	$(4,3)$	$(8,7)$	$(4,4)$/FBMC
$SIR[dB]$	43.7	39.9	36.8	34.0	43.8	40.1	36.7	35.7	34.0
$\eta[bit/s/Hz]$	1	1.5	2	2	1.25	2	2.75	3	3

- Subcarrier frequency separation: $F_0 = 15KHz$
- Symbol duration: $T = 1/15000s$
- FFT/IFFT size: $M = 1024$
- Modulation mode: QPSK(N=4)/8PSK(N=8)
- Carrier frequency: $F_c = 1GHz$
- Mobile's moving speed: $v = 90km/h$

The 3GPP LTE standardized Extended Vehicular A (EVA) channel [14] is adopted in our simulations. The channel information is assumed to partly known at the receiver, with the doppler frequency still existing when we employ an optimal ML detector to detect the transmit symbol. For the FBMC specified parameters: the EGF (Extended Gaussian Function) [15] is adopted in our simulation with overlapping factor $K = 8$ and $\alpha = 2$.

The SIR improvement is shown in table III, and Fig.6 shows the BER performance of the FBMC system and the FBMC-IM system for QPSK and 8PSK. The subblock size Q is set to 4 or 8 and the number of active subcarriers in each subblock k is set to $1, 2, 3$ or 7. η denotes the spectral efficiency, which is defined as $(p_1 + p_2)/Q$. It can be observed that the less of the number of active subcarriers, the higher SIR and the better BER performance will be achieved. And the SIR gain in table III is consistent with that in Fig.6. Only when $(Q, k) = (4, 3)$ for QPSK modulation and $(Q, k) = (8, 7)$ for 8PSK modulation, the FBMC-IM system has the same spectral efficiency with the FBMC system. But the FBMC-IM system performs better compared with the conventional FBMC system. Although it is at the cost of loss in spectral efficiency for other (Q, k), the index modulation shows its superiority in performance when combined with FBMC system for both QPSK and 8PSK. When the modulation mode is 8PSK, the FBMC system shows error floor because of the doppler. By applying index modulation to FBMC system, the error floor disappears gradually as the k becomes smaller.

The BER performance of the FBMC-IM system without optimization and the FBMC-IM system with optimization is presented in Fig.7, where the Comb. Chos. curve is the BER from p_2G, the Comb. Map. curve is the BER from p_1G and the FBMC-IM curve is the BER of the FBMC-IM system, respectively. The modulation mode is QPSK for Fig.7. After selecting the optimal combinations and following the optimal mapping rule, the FBMC-IM system with optimization performs better than that without optimization. And the larger of Eb/N0, the superiority of the optimal algorithm becomes more obvious. This is consistent with the theoretical analysis in BER improvement.

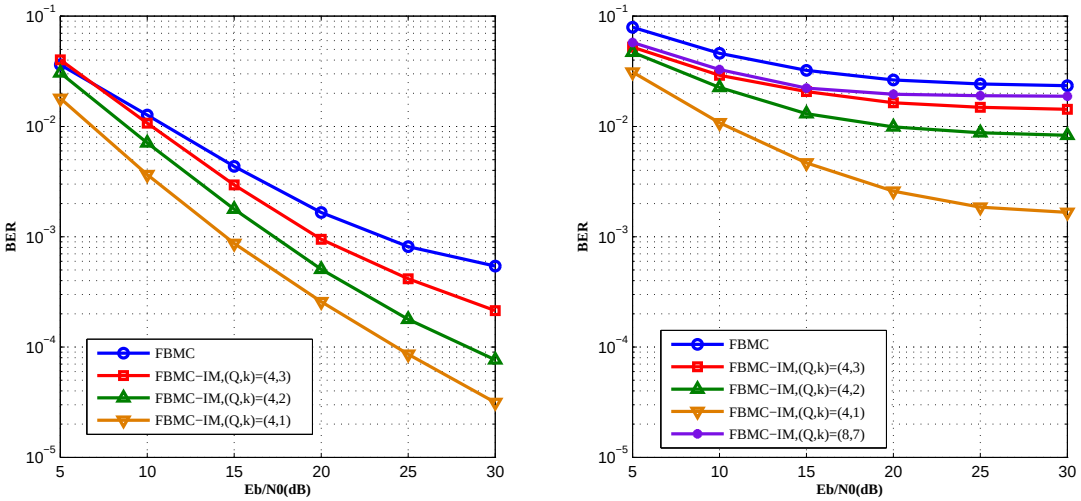

Fig. 6. BER comparison of the conventional FBMC system and the FBMC-IM system, with QPSK (left) and 8PSK (right)

With the group number Q grows larger, there exists performance degradation in combination-selection algorithm. This can be explained with the fact that we only abandon the combinations whose error probability is the largest. However, The number of error bits will be large if there exists the second largest error probability combinations when Q grows larger. Besides, there also exists performance degradation in combination-mapping rule. This is the reason that more bits are carried by the indices of subcarriers when Q grows larger. When the modulation mode changes to 8PSK, the BER improvement remains the same, which is evidenced by the results shown in Fig.8.

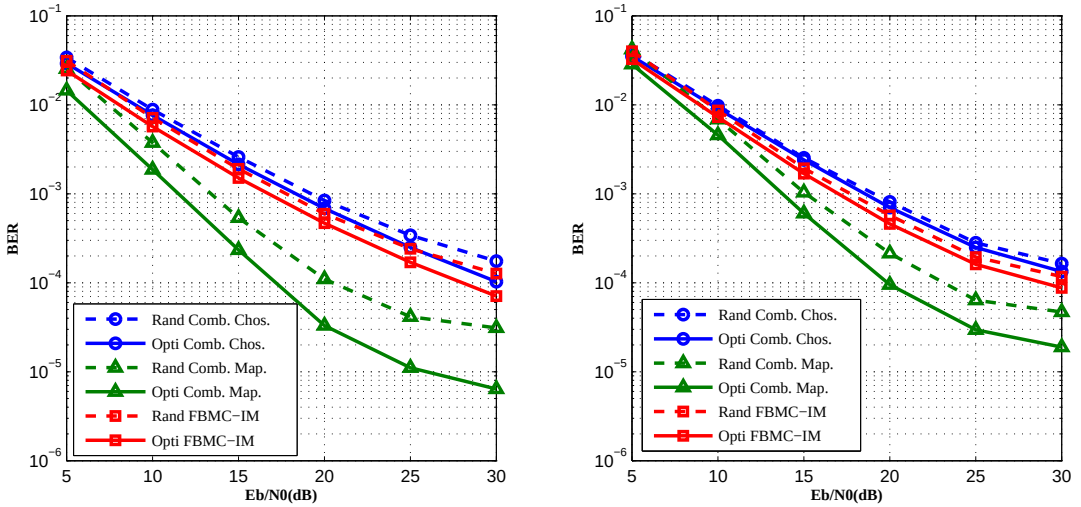

Fig. 7. BER comparison of the FBMC-IM system without optimization and the FBMC-IM system with optimization, with (Q,k)=(4,2) (left) and (Q,k)=(6,3) (right)

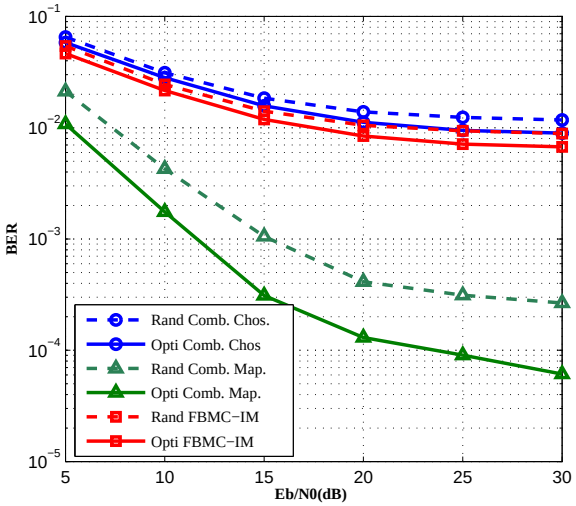

Fig. 8. BER comparison of the FBMC-IM system without optimization and the FBMC-IM system with optimization, (Q,k)=(4,2) for 8PSK

VII. CONCLUSION

In this paper, we introduce index modulation to the FBMC system, and a better SIR and BER performance can be achieved compared with the conventional FBMC system. After that, an optimal combination-selection algorithm and an optimal combination-mapping rule for the FBMC-IM system are presented. By selecting the optimal combinations from all of the combinations, using Gray code constellation to map the combinations to specified bits and considering the maximum Hamming distance, a better BER performance of FBMC-IM system can be achieved. The theoretical analysis and simulation results show the superiority of the FBMC-IM system in BER performance under double-dispersive channels. The optimization of the combinations with which independent index modulation is performed on the in-phase and quadrature component per subcarrier will be researched in the future.

REFERENCES

[1] Farhang-Boroujeny, B. : 'OFDM versus filter bank multicarrier', IEEE Signal Processing Magazine, 2011, 28, (3), pp. 92-112.

[2] 5GNOW: 'D3.1: 5G waveform candidate selection', 2013.

[3] Bellec, M., Pirat, P. : 'OQAM performances and complexity', IEEE P802.22 Wireless Regional Area Network, Jan. 2006.

[4] Bai, Q., Nossek, J. : 'On the effects of carrier frequency offset on cyclic prefix based OFDM and filter bank based multicarrier systems', Signal Processing Advances in Wireless Communications (SPAWC), June 2010, pp. 1-5.

[5] Mesleh, R., Haas, H., Sinanovic, S., et al. : 'Spatial modulation', IEEE Trans. Veh. Technol., 2008, 57, (4), pp. 2228-2241.

[6] Abualhiga, R., Haas, H. : 'Subcarrier-index modulation OFDM', Proc. IEEE Int. Symp. Pers., Indoor Mobile Radio Commun., Tokyo, Japan, September 2009, pp. 13-16.

[7] Tsonev, D., Sinanovic, S., Haas, H. : 'Enhanced subcarrier index modulation (SIM) OFDM', Proc. IEEE GLOBECOM Workshops, Houston, USA, December 2011, pp. 728-732.

[8] Basar, E., Aygolu, U., Panayirci, E., et al. : 'Orthogonal frequency division multiplexing with index modulation', IEEE Trans. Signal Process., 2012, 61, (22), pp. 5536-5549.

[9] Xiao, Y., Wang, S. Dan, L., et al. : 'OFDM with interleaved subcarrier-index modulation', IEEE Commun. Lett., 2014, 18, (8), pp. 1447-1450.

[10] Fan, R., Yu, Y., Guan, Y. : 'Generalization of orthogonal frequency division multiplexing with index modulation', IEEE Trans. Wireless Commun., 2015, 14, (10), pp. 5350-5359.

[11] Lin, H., Gharba, M., Siohan, P. :'Impact of time and carrier frequency offsets on the FBMC/OQAM modulation scheme', Signal Processing, 2014, 102, pp. 151-162.

[12] Farhang-Boroujeny B., Yuen, C. H. : 'Cosine modulated and offset QAM filter bank multicarrier techniques: A continuous-time prospect', EURASIP J Appl Signal Process, 2010, 2010, (6).

[13] Lin, H., Siohan, P., Tanguy P., et al. : 'An Analysis of the EIC Method for OFDM/OQAM Systems', Journal of Communications, 2009, 4, (1), pp. 52-60.

[14] Dahlman, E., Parkvall, S., Skold, J. : '4G: LTE/LTE-Advanced for Mobile Broadband', Academic Press, 2011.

[15] Siohan, P., Roche, C. : 'Cosine-modulated filterbanks based on extended Gaussian functions', IEEE Transactions on Signal Processing, 2000, 48, (11), pp. 3052-3061.